CENTRAL ASIAN JOURNAL OF MATHEMATICAL THEORY AND COMPUTER SCIENCES
https://cajmtcs.centralasianstudies.org/index.php/CAJMTCS
Volume: 06 Issue: 01 | January 2025 ISSN: 2660-5309

.

Article

Enhanced Classification of Damaged Solar Cells Using Transfer Learning with Pre-Trained Networks

Maha Safar Abdulmajed[1], Khalid Saeed Al-badri[2]

1. Department of Laboratory Sciences, College of Pharmacy, University of Tikrit, Tikrit, Iraq
2. Department of Physics, College of Education, University of Samarra, Iraq

Abstract: Among renewable resources, solar power is the most necessary one. Unfortunately, the performance of solar panels depends to a great extent on their components, particularly damagedsolar cells, which can also result in possible failure of the system. Early detection of these defects is important in order to maintain solar energy systems efficiently. Electroluminescence imaging has emerged as a powerful technique for quickly identifying defects in photovoltaic cells, and new developments in deep learning have enabled the automation of this diagnostic process. In this work, we implemented transfer learning on three popular convolutional neural networks: ResNet50, VGG16, and InceptionV3. They were to be classified based on images taken from electroluminescence, the goal of the I hold talons. We relied on a publicly.

Keywords: Artificial intelligence, Transfer Learning, ResNet50, VGG16, InceptionV3, Electroluminsecence

Citation: Abdulmajed, M. S., Al-badri, K. S. Enhanced Classification of Damaged Solar Cells Using Transfer Learning with Pre-Trained Networks. Central Asian Journal of Mathematical Theory and Computer Sciences 2025, 6(1), 76-84.

Received: 10th Jan 2024
Revised: 23th Jan 2024
Accepted: 31th Jan 2025
Published: 12th Feb 2025

1. Introduction

Green energy has become a necessity and a growing demand in today's world. One of its key benefits is that it is environmentally friendly and often more cost-effective compared to traditional energy sources [1], [2], [3]. Solar energy, in particular, stands out as a primary method for generating electricity that is both sustainable and free from harmful environmental impacts [4], [5], [6]. As a result, the demand for solar panels, which produce clean and renewable energy, has surged in the market [7], [8]. Solar panels, which are often robot assembled, are produced on a large scale and need to pay close attention to manufacturing and maintenance processes [9]. However, even solar panels aren't free from defects despite progress. One of the common issue is broken panel cells : It leads to panel failure. Manually identifying and repairing these damaged cells is tedious, complicated and can be human error-prone [10], [11], [12]. What's more, the emergence of technology, most notably artificial intelligence (AI), holds great potential to address these types of challenges. Deep learning, a subset ofof AI, has proven especially effective in tasks like image classification, making it a valuable tool for detecting defects in solar panels [13].

System designs have been proposed for incorporating different methods for inspecting and identifying faulty solar panels [14], [15]. Common techniques for solar panel cell classification include electroluminescence (EL) imaging, infrared (IR) imaging, and RGB imaging [16], [17], [18]. Of these techniques, electroluminescence imaging has proven to be significantly more effective than conventional methods, such as charge-coupled device (CCD) imaging, in assessing photovoltaic (PV) systems [19], [2], [21]. Deep learning algorithms have also shown promising capability to address challenging computer vision problems, such as image classification [12], [22], [23], [24].

In this study we applied deep learning methods, namely convolutional neural networks (CNNs), to classify damaged PV cells from electroluminescence based imaging. We also used transfer learning, which uses a model learned from a large dataset to tell apart damaged from healthy cells. This builds on earlier work 1 which employed a pre-trained model of the common VGG16 model on remote sensing images to classify damaged solar cells [25]. Lightweight CNN for identification of hotspots and damage area in PV cell [26] Modified U-Net networks have been employed by some researchers to classify and identify the damaged solar cells [27], and a few have proposed multispectral neural networks, achieving accuracy as high as 94% [28]. Deep learning is another approach, used for feature extraction to classify the damaged parts of solar panels [29]. For example, AlexNet architecture was customized for fault classification [30], and CNNs have been used for detecting fault patterns [31]. In a study of five different CNN-based networks, the authors were able to achieve an impressive accuracy of 98% when classifying damaged solar cells [32]. In our study, we tested how well CNNs can classify images of non-defective or defective solar cells. We used transfer learning with pre-trained models such as ResNet50, VGG16, InceptionV3 We utilized a public dataset and split it into train, validation, and test sets. The experiments were conducted using Google Colab, which provided free access to GPU resources for processing. This approach allowed us to efficiently analyze and classify damaged solar cells, contributing to the ongoing efforts to improve solar panel reliability and performance.

2. Materials and Methods

2.1. Dataset

In this study, we used defective solar cells to classify them based on electroluminescence images. The dataset was divided into two main categories: "Normal" and "Defective." A total of 2,624 images were used, each with a resolution of 300x300 pixels. All the images are 8-bit grayscale and are publicly available on Kaggle [33]. Figure 1 provides examples of images from this dataset. The dataset was then split into training and testing sets. For testing, 1,177 images (both defective and normal) were used, while 135 images (also a mix of defective and normal) were reserved for evaluation. To further refine the process, the training dataset was divided into train and validation subsets. These subsets were used to monitor the loss graphs, which are discussed in detail in Section 3. The evaluation of the models—ResNet50, VGG16, and InceptionV3—was conducted using the testing dataset. This approach allowed us to assess the performance of these models in accurately classifying defective solar cells.

2.2. The methodology of stady

Figure 2 illustrates the proposed_model employed for the technique of transfered learning TL aimed at identifying and classifying defective solar panels. The primary goal of this model is to categorize input images into two distinct groups: normal and damaged. The process involves two key stages. First, data preparation is crucial, which includes enhancing the data and normalizing the pixel values. The second stage focuses on classification, where we utilize the trained models—ResNet50, VGG16, and InceptionV3—to perform the actual identification of defects.

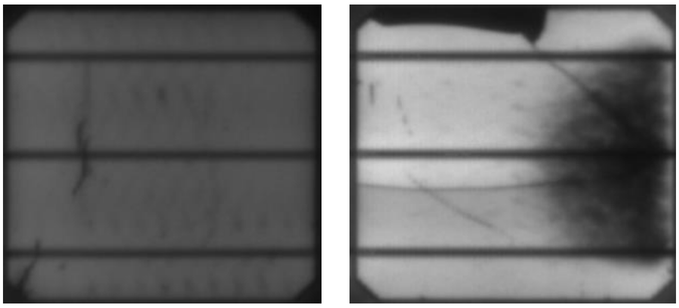

(a) (b)

Figure 1. Samples from the dataset [33] (a) Defected solar cell and (b) Normal solar cell.

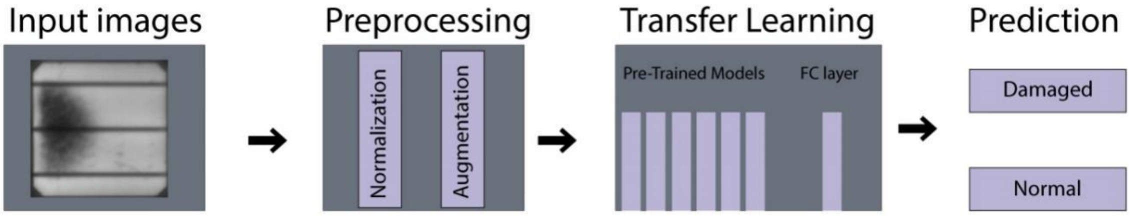

Figure 2. The methodology of TL of classification of solar panls.

Normalization and data augmentation are the next two processes in the data preprocessing process. During normalising, the picture pixels were shrunk to a range between 0 and 1. The dataset's photos were rescaled by multiplying each one by 1/255. While techniques like 1) a 30 degree rotation, and 2) vertical and horizontal flipping were used to supplement the data. Figure 3 illustrates augmented images.

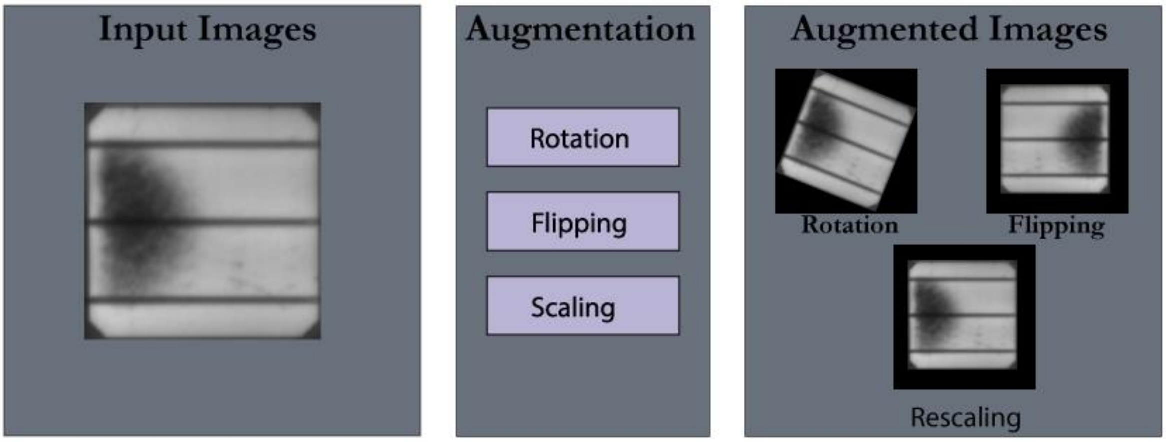

Figure 3. Presented the data-augmentation applied on the soler panals.

Table 1. The parameter that are used on Pre-trained.

Mod.	Layers	Values (million)	I/P layer size	O/P layer size
ResNet50	50	23	224, 224, 3	2,1
VGG16	16	135	224, 224, 3	2,1
Inception V3	48	23.9	224, 224, 3	2,1

2.3. Transfer learning using Pre-trained Models

Convolutional neural network (CNN) models have proven to be highly effective for classifying and processing images . However, training these CNN models from scratch can be quite challenging due to the limited availability of image datasets [34]. Transfer learning offers a solution by allowing a deep learning model that has been trained on a larger dataset to apply its knowledge to tasks involving smaller datasets. In this study, we distinguished between damaged and healthy cells using pre-trained models, specifically ResNet50, VGG16, and InceptionV3. The architectural details of these models are presented in Table 1.

These pre-trained models have already undergone training on the ImageNet dataset. To implement transfer So, to ensure that the efficiency was the best we could get, we added a dense layer to optimize the training parameters. Furthermore, we added one additional batch normalization layer to discard unassigned neuron weights from the pre-trained models. replace the last dense layers in ResNet50, VGG16, and InceptionV3 with a new fully-connected (FC) layer with two perceptron values for each class. Keep in mind hyperparameters are vital to optimize these pre-trained models.

2.4. Fine tuning and hyperparamters

One of the essential elements on which the model is trained in transfer learning is fine tuning. The image was reduced to 224x224 pixels, Adam optimizers were used, and the following hyperparameters were maintained: momentum was set to 0.95, weight decay was set to 0.0005, batch size was set to 10, and learning rate was set to 0.001 with a factor value of 0.7. Apart from the aforementioned parameters, the model was often having overfitting issues before these parameters were chosen after the model was trained on a variety of values.

3. Results

3.1. Experimental Setup and Performance Metrices

The dataset is assessed using the pre-trained models. Table 2 shows data on the train and test datasets and also applies a 90{10} training-round in order to find ratio. Utilizing the supplemented data, the suggested models have been trained.

Table 2. Data splitting.

Classes	Trian	Valied	Test
Deficted	942	235	135
Narmal	942	235	135
Total	1884	470	270

The images for the training and validation datasets were resized to 224 x 224 pixels. We trained the pre-trained models in batches of 10, with a total of 80 epochs. The batch size and the number of epochs were selected manually based on empirical methods. During training, we set the learning rate for each model to 0.001 and used the Adam optimizer to minimize errors.

To evaluate the quality of the origin V3-model, we used several values, including Spe: Specificity; Pre: Precision; Siv: Sensitivity, F1_Score, and Acu: Accuracy . These metrics were derived from the components of the confusion matrix: True Positive (TP), True Negative (TN), False Positive (FP), and False Negative (FN). The calculations for these metrics were performed using Equations (1)-(6) [35].

$$Pre = \frac{TP}{TP+FP} \quad (1)$$

$$Recall = \frac{TP}{TP+FN} \quad (2)$$

$Siv = \frac{TP}{FN+TP}$ (3)

$Spe = \frac{TN}{FP+TN}$ (4)

$Acu = \frac{TP+TN}{FP+TP+TN+FN}$ (5)

$F1\_score = 2 \text{ x} \frac{Precision\ x\ Recall}{Precision+Recall}$ (6)

In this work, the two important factors $normal$ and $faulty$ were seen as $negative$ and $positive$ categories, correspondingly. The $normal$ and $defective$ classes are thus indicated by the TN and TP, correspondingly. While FN and FP stand for incorrectly classifying expected normal instances and defects, correspondingly.

3.2. Results

The performance of the models has been compared based on metrics such as training loss, validation loss, and validation accuracy for each epoch. The results for these parameters are summarized in Table 3. We evaluated these metrics to assess whether the training models were experiencing overfitting or underfitting.

To further validate performance, we created confusion matrices to classify the data into true positives, true negatives, false positives, and false negatives after training. The confusion matrices for the pre-trained models on the test dataset are presented in Figure 4. We used Equations (1) through (6) to calculate various performance metrics from the data generated by the confusion matrices, including precision, recall, F1 score, sensitivity, specificity, and accuracy. The results for these metrics are displayed in Table 4.

Table 3. Training performance of pre-trained models.

Model	Epochs	Train loss	Valid loss	Train accuracy	Valid accuracy
ResNet50	1	0.812	0.832	68.24	71.42
	.	.	.	.	.
	.	.	.	.	.
	79	0.132	0.123	94.61	93.32
	80	0.131	0.108	94.53	95.63
VGG16	1	0.712	0.794	78.31	73.68
	.	.	.	.	.
	.	.	.	.	.
	79	0.101	0.112	95.23	95.87
	80	0.009	0.102	97.52	96.88
Inception V3	1	0.712	0.842	69.54	70.23
	.	.	.	.	.
	.	.	.	.	.
	79	0.121	0.132	93.71	93.32
	80	0.112	0.181	95.83	95.65

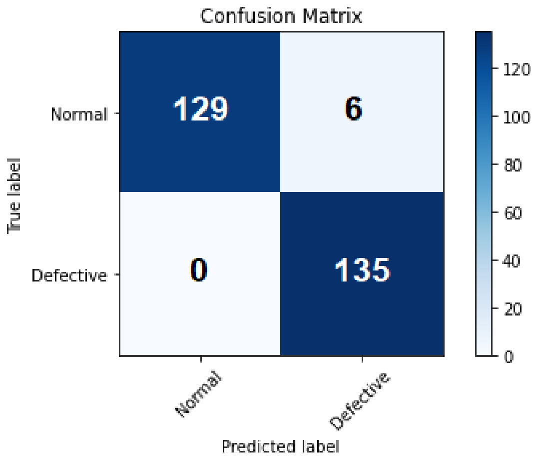

(a)

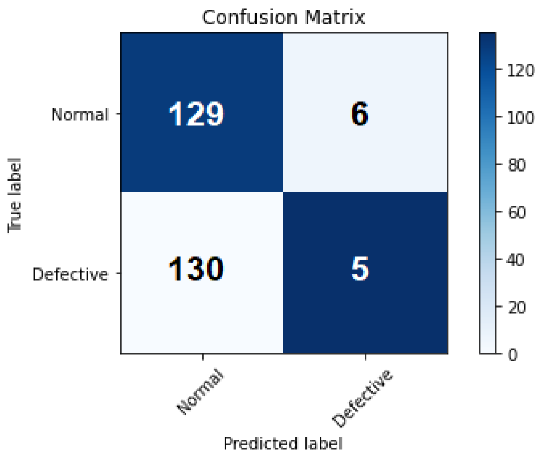

(b)

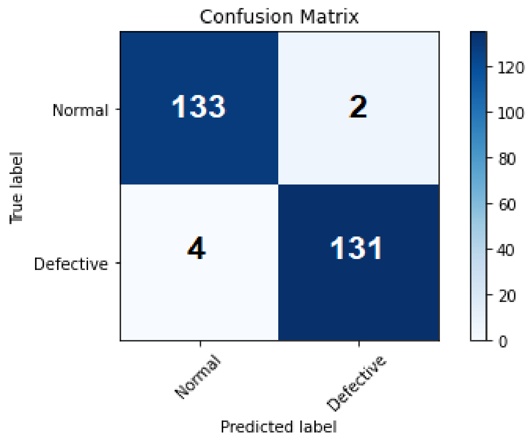

(c)

Figure 4. Confusion metrices achieved on each model for test dataset (a) ResNet50 (b) InceptionV3 (c) VGG16.

Table 4. Performance of the models.

Model	Precision	Recall	F1-Score	Sensitivity	Specificity	Accuracy
ResNet50	97.87	97.82	97.77	97.82	94.07	97.40
VGG16	97.08	96.27	98.52	98.50	97.79	97.78
Inception V3	95.56	96.27	95.51	96.27	95.59	95.93

3.2.1. Comparison with different optimizers

VGG16 model which outperformed the rest of the models have been tested with various optimizers such as RMSProp, Adadelta, SGD, and Adam, in order to do the comparison of the accuracies on the testing datasetThe Adam optimizer produced the most promising results out of all the optimizers. Thus, Adam optimizer was chosen to train the model. Table 5 presents the values based on Adam optimizer.

Table 5. Shows the VGG16 performance for different optimizer.

Model	Optimizer	Precision	Specifity	Sensitivity	F1-score	Accuracy
VGG16	Adam	97.0	96.2	98.5	98.5	97.7
	SGD	83.0	89.0	95.2	0.89	90.3
	Adadelta	92.3	91.4	92.1	0.92	92.1
	RMSProp	95.6	92.3	94.7	0.94	95.5

3.2.2. Comparison with different batch size

One key hyper-parameter for Deep Neural Networks is batch size, according to experts. This study shows values based on various batch sizes. Table6 presents the accuracy results obtained after training on various batch sizes, from 8 to12. It has been noted that a batch size of 10 results in improved testing performance. Thus all the models has been trained using batches of 10.

Table 6. Testing accuracies on different batch sizes on ResNet50.

Model	Batch size		
VGG16	8	10	12
	85.27%	97.78%	90.25%

4. Discussion

Future work

This discovery has opened the door to the development of highly efficient deep neural networks that can quickly and accurately detect damaged solar cells. The proposed model is anticipated to perform exceptionally well in distinguishing between defective and healthy solar cells, which will significantly enhance fault detection in photovoltaic systems.

Looking forward, the capabilities of this model could be expanded beyond simple binary classification to identify various types of solar cell defects. This would create a more comprehensive diagnostic framework. By incorporating a wider range of datasets and real-world conditions, we can further refine the model to improve its robustness and ability to generalize across different solar panel technologies.

Moreover, combining sophisticated optimization methods with deep neural networks (DNNs) may result in stronger and more effective models. Techniques such as hyperparameter tuning, feature selection, ensemble learning, and reinforcement learning could improve the accuracy and reliability of the classification of solar cells. In addition, we believe this model can progressively benefit from explainable AI (XAI) techniques to provide insights into how the decision making has been made, hence enhancing trust and usability in industrial applications.

Future studies can determine deploying these models into edge computing devices or Internet of Things (IoT) frameworks in real-time. This would allow for fault detection on-site without the need for cloud-computing-based processing. These advancements will allow solar panel monitoring systems to be more cost-effective, scalable, and versatile, supporting the wider sprawl of smart renewable energy solutions.

5. Conclusion

We interpolated deep learning modes such as ResNet50, VGG16, and InceptionV3 for image parameterization of destroyed solar cells in classification. The training was done on a dataset containing 2,624 images of defective and healthy solar cells. In addition, we considered various performance metrics like sensitivity, specificity, F1-score, precision, recall, loss graphs and confusion matrices to properly analyze the performance of the model. Such metrics offered a complete comprehensive assessment of classification performance, comprehensively evaluating the models reliability and the ability of the models to accurately identify a faulty solar cell. Of all models, VGG16 demonstrated the strongest classification performance, successfully separating images of damaged and normal solar cells. The accuracy for VGG16, ResNet50, and InceptionV3 were 97.78%, 97.40%, and 95.93% respectively, indicating the statistic of deep learning mode is high. We further experimented with different optimization techniques to improve the model's learning capabilities. This allowed testing of several optimizers and the Adam optimizer yielded the best convergence and accuracy across all deep neural networks (DNNs) tested. It is one of the most successful algorithms that helped increase the efficiency of the model in the function of adaptive learning rates in the process of optimizing the learning process of deep neural networks equipped with the gradient descent method.

REFERENCES

[1] D. Matusz-Kalász and I. Bodnár, "Monitoring and Diagnostics of Photovoltaic Cells by Electroluminescence," in 2022 23rd International Carpathian Control Conference (ICCC), 2022, pp. 158-161: IEEE.

[2] M. Farhan Bashir, M. Sadiq, B. Talbi, L. Shahzad, and M. Adnan Bashir, "An outlook on the development of renewable energy, policy measures to reshape the current energy mix, and how to achieve sustainable economic growth in the post COVID-19 era," Environmental Science and Pollution Research, pp. 1-12, 2022.

[3] D. Asante et al., "Prioritizing strategies to eliminate barriers to renewable energy adoption and development in Ghana: A CRITIC-fuzzy TOPSIS approach," Renewable Energy, vol. 195, pp. 47-65, 2022.

[4] A. I. Almulhim, "Understanding public awareness and attitudes toward renewable energy resources in Saudi Arabia," Renewable Energy, vol. 192, pp. 572-582, 2022.

[5] A. Rahman, O. Farrok, and M. M. Haque, "Environmental impact of renewable energy source based electrical power plants: Solar, wind, hydroelectric, biomass, geothermal, tidal, ocean, and osmotic," Renewable and Sustainable Energy Reviews, vol. 161, p. 112279, 2022.

[6] A. Q. Al-Shetwi, "Sustainable development of renewable energy integrated power sector: Trends, environmental impacts, and recent challenges," Science of The Total Environment, p. 153645, 2022.

[7] M. Valizadeh, I. R. N. ALRubeei, H. T. S. ALRikabi, and F. T. Abed, "Enhancing the efficiency of photovoltaic power system by submerging it in the rivers," Telkomnika (Telecommunication Computing Electronics and Control), vol. 20, no. 1, pp. 166-172, 2022.

[8] J. Zhao, K. Dong, X. Dong, and M. Shahbaz, "How renewable energy alleviate energy poverty? A global analysis," Renewable Energy, vol. 186, pp. 299-311, 2022.

[9] M. Dahl, "Development of Structures and Methods for Safe On Orbit Robotic Assembly of Small Satellites," Massachusetts Institute of Technology, 2022.

[10] Ł. Paśko et al., "Plan and Develop Advanced Knowledge and Skills for Future Industrial Employees in the Field of Artificial Intelligence, Internet of Things and Edge Computing," vol. 14, no. 6, p. 3312, 2022.

[11] P. C. Johnson, C. Laurell, M. Ots, C. J. T. F. Sandström, and S. Change, "Digital innovation and the effects of artificial intelligence on firms' research and development–Automation or augmentation, exploration or exploitation?," vol. 179, p. 121636, 2022.

[12] M. Umair et al., "Detection of COVID-19 Using Transfer Learning and Grad-CAM Visualization on Indigenously Collected X-ray Dataset," vol. 21, no. 17, p. 5813, 2021.

[13] A. Mujkić, E. Baralić, A. Ombašić, L. S. Bećirović, L. G. Pokvić, and A. Badnjević, "Machine Intelligence in Biomedical Data Modeling, Processing, and Analysis," in 2022 11th Mediterranean Conference on Embedded Computing (MECO), 2022, pp. 1-10: IEEE.

[14] M. Vlaminck, R. Heidbuchel, W. Philips, and H. J. S. Luong, "Region-Based CNN for Anomaly Detection in PV Power Plants Using Aerial Imagery," vol. 22, no. 3, p. 1244, 2022.

[15] A. Raorane, D. Magare, and Y. Mistry, "Performance of fault classification on Photovoltaic modules using Thermographic images," in ITM Web of Conferences, 2022, vol. 44, p. 03065: EDP Sciences.

[16] I. Høiaas et al., "Inspection and condition monitoring of large-scale photovoltaic power plants: A review of imaging technologies," vol. 161, p. 112353, 2022.

[17] C. Buerhop, L. Bommes, J. Schlipf, T. Pickel, A. Fladung, and M. J. P. i. E. Peters, "Infrared imaging of photovoltaic modules A review of the state of the art and future challenges facing gigawatt photovoltaic power stations," 2022.

[18] X. Chen, T. Karin, and A. J. S. E. Jain, "Automated defect identification in electroluminescence images of solar modules," vol. 242, pp. 20-29, 2022.

[19] O. A. Alimi, E. L. Meyer, and O. I. J. E. Olayiwola, "Solar Photovoltaic Modules’ Performance Reliability and Degradation Analysis—A Review," vol. 15, no. 16, p. 5964, 2022.

[20] R. Singh, M. Sharma, and K. J. R. E. Yadav, "Degradation and reliability analysis of photovoltaic modules after operating for 12 years: A case study with comparisons," vol. 196, pp. 1170-1186, 2022.

[21] K. SAEED-UZ-ZAMAN, "Effect of Charge Transfer State Energetic Disorder on Spectral Response, Recombination and Energy Loss of Organic Solar Cells," 2022.

[22] H. M. Ahmad and A. J. J. o. M. S. Rahimi, "Deep learning methods for object detection in smart manufacturing: A survey," vol. 64, pp. 181-196, 2022.

[23] F. Kulsoom, S. Narejo, Z. Mehmood, H. N. Chaudhry, A. K. J. N. C. Bashir, and Applications, "A review of machine learning-based human activity recognition for diverse applications," pp. 1-36, 2022.

[24] M. E. Salman, G. Ç. Çakar, J. Azimjonov, M. Kösem, and İ. H. J. E. S. w. A. Cedi̇moğlu, "Automated prostate cancer grading and diagnosis system using deep learning-based Yolo object detection algorithm," vol. 201, p. 117148, 2022.

[25] R. Pierdicca et al., "DEEP CONVOLUTIONAL NEURAL NETWORK FOR AUTOMATIC DETECTION OF DAMAGED PHOTOVOLTAIC CELLS," vol. 42, no. 2, 2018.

[26] M. W. Akram et al., "CNN based automatic detection of photovoltaic cell defects in electroluminescence images," vol. 189, p. 116319, 2019.

[27] M. R. U. Rahman and H. J. I. A. Chen, "Defects inspection in polycrystalline solar cells electroluminescence images using deep learning," vol. 8, pp. 40547-40558, 2020.

[28] H. Chen, Y. Pang, Q. Hu, and K. J. J. o. I. M. Liu, "Solar cell surface defect inspection based on multispectral convolutional neural network," vol. 31, no. 2, pp. 453-468, 2020.

[29] X. Li, Q. Yang, Z. Lou, and W. J. I. T. o. E. C. Yan, "Deep learning based module defect analysis for large-scale photovoltaic farms," vol. 34, no. 1, pp. 520-529, 2018.

[30] F. Aziz, A. U. Haq, S. Ahmad, Y. Mahmoud, M. Jalal, and U. J. I. A. Ali, "A novel convolutional neural network-based approach for fault classification in photovoltaic arrays," vol. 8, pp. 41889-41904, 2020.

[31] X. Li, Q. Yang, J. Wang, Z. Chen, and W. J. J. S. C. I. Yan, "Intelligent fault pattern recognition of aerial photovoltaic module images based on deep learning technique," vol. 16, pp. 67-71, 2018.

[32] G. Cipriani, A. D’Amico, S. Guarino, D. Manno, M. Traverso, and V. J. E. Di Dio, "Convolutional neural network for dust and hotspot classification in PV modules," vol. 13, no. 23, p. 6357, 2020.

[33] "Defective Solar Cells (Electroluminescence Images)," ed, 2022.

[34] G. Liang, H. Hong, W. Xie, and L. J. I. A. Zheng, "Combining convolutional neural network with recursive neural network for blood cell image classification," vol. 6, pp. 36188-36197, 2018.

[35] S. R. Nayak, D. R. Nayak, U. Sinha, V. Arora, and R. B. Pachori, "Application of deep learning techniques for detection of COVID-19 cases using chest X-ray images: A comprehensive study," Biomedical Signal Processing and Control, vol. 64, p. 102365, 2021/02/01/ 2021.